

# Design method of a vertical screw conveyor based on Taylor–Couette–Poiseuille stable helical vortex

Advances in Mechanical Engineering  
2017, Vol. 9(7) 1–11  
© The Author(s) 2017  
DOI: 10.1177/1687814017714984  
[journals.sagepub.com/home/ade](http://journals.sagepub.com/home/ade)  


Sun Xiaoxia, Meng Wenjun and Yuan yuan

## Abstract

This article investigates gas–solid two-phase flow in a vertical screw conveyor and analyzes the distribution function of the circumferential velocity of particles in the radial direction. Theoretical analysis combined with EDEM + FLUENT simulation analysis is performed to determine the best fill rate, the best screw speed, and critical Reynolds number when Taylor–Couette–Poiseuille flow stable helical vortex forms in the vertical screw conveyor. The formula for the critical Reynolds number and the best throughput is determined under different friction coefficients to establish an efficient design method based on Taylor–Couette–Poiseuille stable helical vortex flow. The method greatly benefits the design of vertical screw conveyors.

## Keywords

Vertical screw conveyor, gas–solid two-phase flow, the Reynolds number, Taylor–Couette–Poiseuille flow stable helical vortex

Date received: 9 January 2017; accepted: 17 May 2017

Academic Editor: Yangmin Li

## Introduction

The vertical screw conveyor is a type of conveyor without flexible traction components. This equipment pushes particles to move through a rotary shaft with a screw blade. In the traditional screw conveying mechanism, the centrifugal force produced by the rotating screw acts on the medium particles, thereby generating friction between the particles and the tube wall. This friction force overcomes the gravitational force of the particles, preventing them from falling.<sup>1,2</sup> Although the structure of the vertical screw conveyor and the conveying principle of the particle are simple, the mechanism of the transport process is very complex. At present, in designing the screw conveyor, performance parameters are determined based only on experience formulas and experimental data, whose method consists mainly of material group and single particle.<sup>3–6</sup> The material group method, with the particle group as the research object, analyzes the theoretical criterion on different

shapes of free surface the material formed in the vertical conveyor. This approach provides a foundation for the design of the screw conveyor, but at the expense of simplifying the established mathematical model and the complexity of experiment, consequently disregarding the role of the gas–solid two-phase flow. Therefore, the mentioned design methods are hindered by these limitations.

The gap in two rotating concentric cylinders produces a secondary flow (Taylor vortex), which is known as the Taylor–Couette (TC) flow.<sup>7–9</sup> Various complex patterns are produced because of the differing radius

College of Mechanical Engineering, Taiyuan University of Science and Technology, Taiyuan, P.R. China

## Corresponding author:

Meng Wenjun, College of Mechanical Engineering, Taiyuan University of Science and Technology, Taiyuan 030024, Shanxi, P.R. China.  
Email: 860115787@qq.com



Creative Commons CC-BY: This article is distributed under the terms of the Creative Commons Attribution 4.0 License (<http://www.creativecommons.org/licenses/by/4.0/>) which permits any use, reproduction and distribution of the work without

further permission provided the original work is attributed as specified on the SAGE and Open Access pages (<https://us.sagepub.com/en-us/nam/open-access-at-sage>).

ratios, rotating angular velocities, and fluid characteristics of the two concentric cylinders.<sup>10</sup> When the outer cylinder is stationary, the flow moves circularly in the horizontal plane around the cylindrical axis if the inner cylinder rotates at a low rotating speed; this movement is called the basic Couette flow. When the angular velocity of the inner cylinder reaches a critical value, the Couette flow begins to lose stability. Then, a new axisymmetric steady flow emerges and reverses the vortex along the axial direction and adjacent vortex. The flow above is called the TC flow, which moves along the circumferential direction only without an axial direction. If an axial force is exerted on the movement, the TC flow simultaneously achieves circumferential speed and axial speed, and this phenomenon is called the Taylor–Couette–Poiseuille (TCP) flow.<sup>11–14</sup> As the Reynolds number is increased, TCP flow can produce various vortices, such as laminar Taylor vortex, stable helical vortex (SHV), and fluctuant helical vortex.<sup>15–17</sup> The radial velocity of the Taylor–Couette–Poiseuille stable helical vortex (TCP-SHV) flow is 0, which contributes to the sucking in of the granular media into the screw conveyor. Consequently, an extremely high-density gas–solid two-phase flow is generated, greatly improving the conveying efficiency. As the Reynolds number increases further, the flow will produce a wide range of disorders, resulting in a turbulent flow.

In a vertical screw conveyor having a screw blade with a high rotation speed, when the particle is small, the interaction between the particles and the air is not ignored, resulting in more complex movements of the particle. G Yuhang<sup>18</sup> simulated the gas phase flow field in the conveyor to obtain the distribution of the gas flow velocity and pressure, and the large axial velocity and tangential velocity can help to lift materials. The existing theory of the vertical screw conveyor ignores the gas–solid two-phase flow under the action of high-speed rotating screw, thus forming a TCP-SHV in vertical screw conveyor. The flow field properties are helpful in improving the transmission efficiency of particles. Once a TCP-SHV flow is formed in the vertical screw conveyor, particles can be effectively transported with reduced power consumption. Once the TCP-SHV flow is broken, the power consumption increases and the throughput is reduced; such a situation is unfavorable for particle transport.

By combining theoretical analysis with EDEM + FLUENT simulation analysis, this article determines the best filling rate, the best screw speed, and the critical Reynolds number when a TCP-SHV flow is formed in the vertical screw conveyor to obtain an efficient design method based on TCP-SHV. The developed method would be greatly beneficial to the design of the vertical screw conveyor.

The applicability and validity of EDEM + FLUENT simulation analysis have been affirmed by

Owen and Cleary,<sup>19</sup> S Xinyu,<sup>20</sup> Z Xiansheng,<sup>21</sup> S Xiaoxia and M Wenjun,<sup>22</sup> and so on. In these articles, the obtained simulation data were very close to the experimental data, and the error was within an acceptable range. To ensure that the screw axis has good rigidity, the shaft radius of the model established in this article is 0.3 times of the screw radius.

## Average circumferential velocity of the particle and the throughput

### Analysis of particle velocity

Figure 1 shows the analysis of the particle velocity in the vertical screw conveyor. As shown, the absolute motion of the particle  $v_A$  was synthesized from two kinds of motion: the rotary motion  $v_s$  rotating the screw axis and the relative motion  $v_R$  between the direction of the screw line and the screw leaf. The absolute speed of the particle was decomposed into the circumference velocity  $v_T$  and the vertical speed of the particle  $v_L$ . In Figure 1,  $\alpha$  is the screw angle of the blade, and  $\lambda$  is the rise angle of the particle speed.

Let  $\omega$  be the screw rotational speed,  $\omega_s$  be the particle rotational speed,  $S$  be the screw pitch, and  $r$  be the radial position. According to Lei<sup>6</sup>

$$v_s = 2\pi\omega \cdot r \quad (1)$$

$$v_T = 2\pi\omega_s \cdot r \quad (2)$$

$$\begin{aligned} v_L &= (v_s - v_T) \tan \alpha = 2\pi(\omega \cdot r - \omega_s \cdot r) \\ \frac{S}{2\pi r} &= (\omega - \omega_s)S \end{aligned} \quad (3)$$

### Circumferential velocity of the particle

A large part of the energy consumed in the vertical screw conveyor is used for maintaining the circular motion of the particle. In the simulation analysis of the

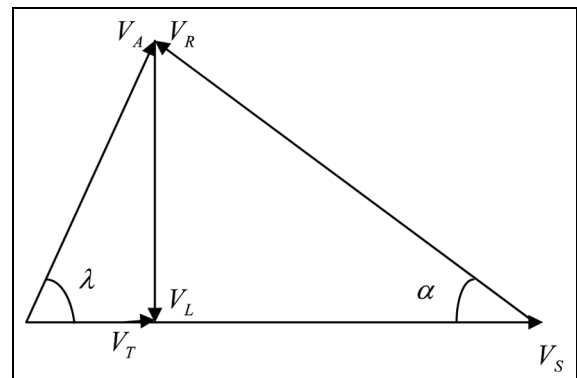
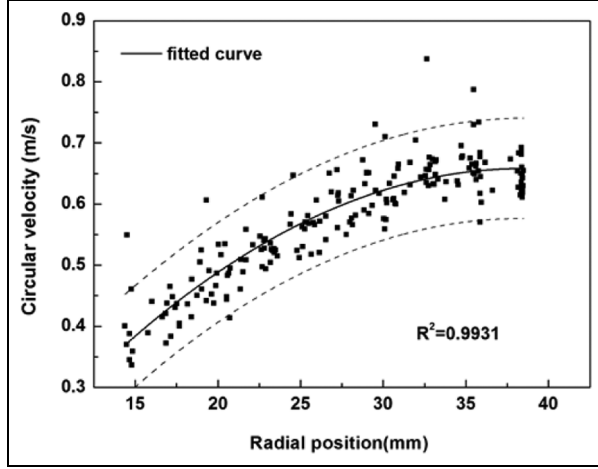
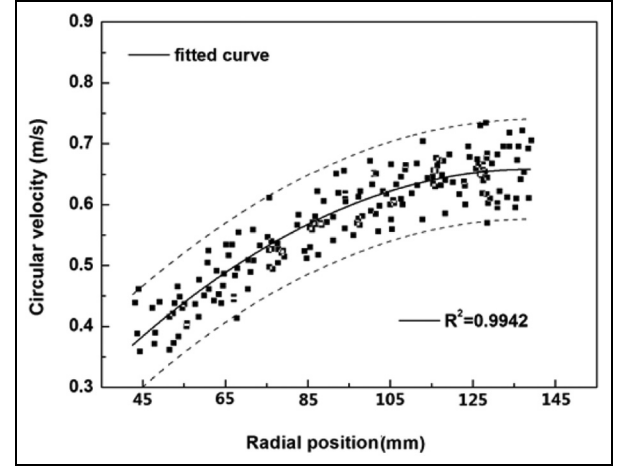


Figure 1. Analysis of the particle velocity.

**Table 1.** The simulation mode of vertical screw conveyor.

| Radius of screw shaft (mm) | Radius of screw (mm) | Screw pitch (mm) | Screw speed (r/s) |
|----------------------------|----------------------|------------------|-------------------|
| 13                         | 40                   | 60               | 8.3               |

**Figure 2.** Regularities of distribution of the circumference velocity of the particle on the radial distribution.**Figure 3.** Regularities of distribution of the circumference velocity of the particle on the radial distribution.

particle flow in the vertical screw conveyor, the built mode is as shown in Table 1.

By the simulation with the above mode, Figure 2 shows the regularities of distribution of the circumference velocity of the particle on the radial distribution. We have fit the simulated data by polynomial fitting function inside the origin software, and the fitted curve function is obtained. The coefficient of determination is 0.9931, which is relatively high. The fitted curve function in the figure is as follows

$$v_T = -0.08 + 38.32r - 498.16r^2 \quad (4)$$

Formula (4) for the circumference velocity of the particle is obtained by the fit function, and then the average rotational velocity of the particle can be obtained. Finally, the formula for the throughput can be obtained.

This fitting function is derived when the screw speed is  $\omega = 8.3 \text{ r/s}$ . The circumference velocity of the particle is linear with the screw speed, which is substituted into the above quadratic fitting function. Thus

$$\begin{aligned} v_T &= \frac{\omega}{8.3} (-0.08 + 38.32r - 498.16r^2) \\ &= \omega (-0.01 + 4.6r - 60r^2) \end{aligned} \quad (5)$$

The preceding analysis reveals that the circumference velocity of the particle is a quadratic function of

the screw radius whose quadratic term coefficient is negative.

When the simulation model is changed with  $R_1 = 45 \text{ mm}$ ,  $R_2 = 150 \text{ mm}$ ,  $S = 1.5$ ,  $R_2 = 225 \text{ mm}$ , and  $\omega = 500 \text{ r/min} = 8.3 \text{ r/s}$ , the regularities of the distribution of the circumference velocity of the particle on the radial distribution are as shown in Figure 3. As shown in Figure 2, a similar fitted quadratic fitting function can be obtained in Figure 3.

According to Figures 2 and 3, the circumference velocities of the particles of the two curves are at their minimum (0.34 m/s) when  $r = R_1$  and at their maximum (90.66 m/s) when  $r = R_2$ .

Therefore, the quadratic function of the circumference velocity of the particle is as follows

$$v_T = \omega \left[ -\frac{0.08}{(0.002 + R_2)^2} (r - R_2)^2 + 0.08 \right] \quad (6)$$

Quadratic function of the throughput

$$2\pi\omega_s r = v_T = \omega \left[ -\frac{0.08}{(0.002 + R_2)^2} (r - R_2)^2 + 0.08 \right] \quad (7)$$

Therefore, the average rotational velocity of the particle is as follows

$$\bar{\omega}_s = \frac{1}{R_2 - R_1} \int_{R_1}^{R_2} \omega_s dr = \frac{0.04\omega}{\pi(R_2 - R_1)} \left( \ln \frac{R_2}{R_1} - \frac{1}{(0.002 + R_2)^2} \cdot \left( \frac{1}{2}(R_2^2 - R_1^2) - 2R_2(R_2 - R_1) + R_2^2 \ln \frac{R_2}{R_1} \right) \right) \quad (8)$$

To maintain the good rigidity of the screw axis, the screw axis radius is set to 0.3 times of the screw radius, that is,  $R_1 = 0.3R_2$ . Substituting this value into the average rotational velocity of the particle yields the following

$$\bar{\omega}_s \approx \frac{0.04\omega(0.00684 + 1.35R_2)}{\pi(0.002 + R_2)^2} \text{ (r/s)} \quad (9)$$

According to Figures 1 and 2, the average vertical velocity of the particle can be obtained as follows

$$\bar{v}_L = (\omega - \bar{\omega}_s)S = \left( 1 - \frac{0.04(0.00684 + 1.35R_2)}{\pi(0.002 + R_2)^2} \right) \omega S \quad (10)$$

**Table 2.** The simulation parameters.

|                 | Parameter                                      | Value      |
|-----------------|------------------------------------------------|------------|
| Particle (coal) | Diameter of particle (mm)                      | 2          |
|                 | Density (kg/m <sup>3</sup> )                   | 1600       |
|                 | Shear modulus (GPa)                            | 1.98       |
|                 | Poisson's ratio                                | 0.5        |
|                 | Particle-particle static friction coefficient  | 0.6        |
|                 | Particle-particle rolling friction coefficient | 0.05       |
|                 | Particle-particle restitution coefficient      | 0.5        |
| Wall (steel)    | The number of particles ( $R_2 = 100$ mm)      | 802,469    |
|                 | The number of particles ( $R_2 = 200$ mm)      | 12,839,506 |
|                 | The number of particles ( $R_2 = 300$ mm)      | 65,000,000 |
|                 | Density (kg/m <sup>3</sup> )                   | 7850       |
|                 | Shear modulus (GPa)                            | 79         |
|                 | Poisson's ratio                                | 0.3        |
|                 | Particle-wall static friction coefficient      | 0.4        |
|                 | Particle-wall rolling friction coefficient     | 0.05       |
|                 | Particle-wall restitution coefficient          | 0.5        |

By substituting formula (10) into the throughput formula, we obtain the following

$$Q = \frac{\pi}{4} (4R_2^2 - 4R_1^2) \phi \rho \bar{v}_L = 0.91 \omega S \rho \phi \pi R_2^2 \left( 1 - \frac{0.04(0.00684 + 1.35R_2)}{\pi(0.002 + R_2)^2} \right) \quad (11)$$

In the preceding equation,  $\rho$  is the bulk density of the particle flow (t/m<sup>3</sup>),  $R_2$  is the screw radius (m),  $\mu_g$  is the coefficient of kinematic viscosity for the air,  $\mu_g = 1.8e - 5$  (m<sup>2</sup>/s),  $\phi$  is the filling rate of the particle flow,  $S$  is the screw pitch (m),  $S = 1.5R_2$ , and  $\omega$  is the screw speed.

Using EDEM + FLUENT simulation analysis to build a model for different screw radii  $R_2$ , the simulation parameters are as shown in Table 2.

The simulation throughput at different screw speeds of 200, 300, and 400 r/min as well as different screw radii of 100, 200, and 300 mm was obtained to verify the correctness of the deduced theoretical throughput, and the experimental data from the work done by Z Zhanyi and Xiaoxia<sup>23</sup> were also used to verify the correctness of theoretical throughput, as shown in Figure 4. The obtained simulation data and experimental data were very close to the theoretical data, and the error was within an acceptable range.

The air velocity at different screw speeds of 200, 300, and 400 r/min with screw radii of 200 mm was obtained, as shown in Figure 5. The speed of the particle and the airflow are in the same direction, but the speed of airflow significantly is greater than the speed of particles. The gas can push the particle transport, which can consider mainly improving vertical speed by distribution of gas-solid two-flow field.

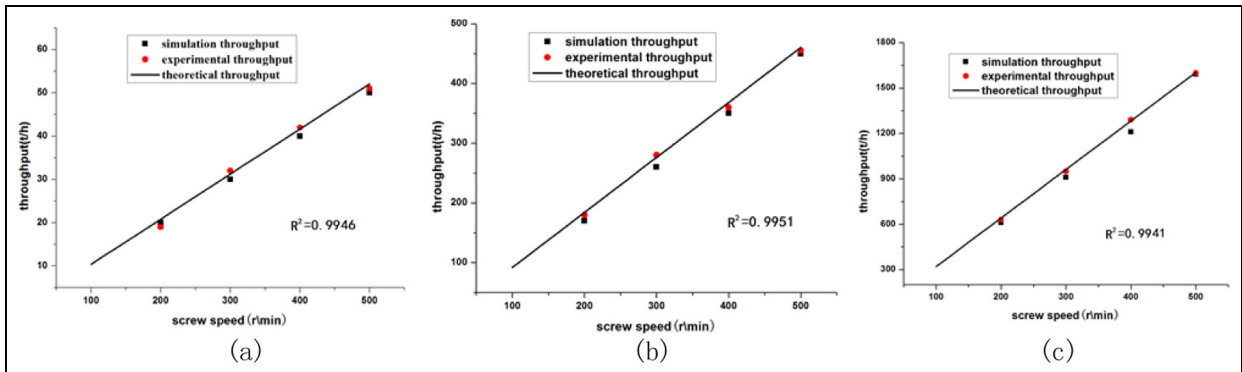


**Figure 4.** Comparison between the theoretical throughput and the simulation throughput under different screw radii and screw speeds: (a)  $R_2 = 100$  mm, (b)  $R_2 = 200$  mm, and (c)  $R_2 = 300$  mm.

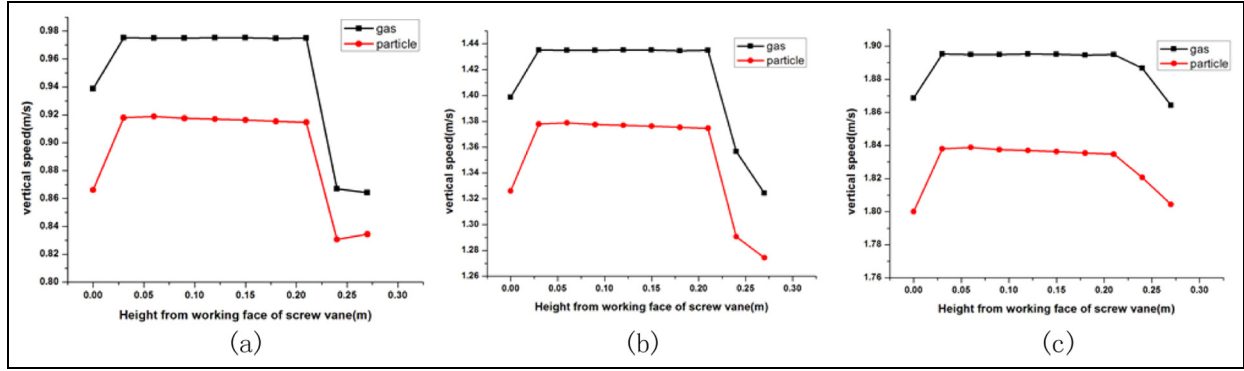


**Figure 5.** Vertical speed of particle and gas, with screw radii of 200 mm: (a)  $\omega = 200$  r/min, (b)  $\omega = 300$  r/min, and (c)  $\omega = 400$  r/min.

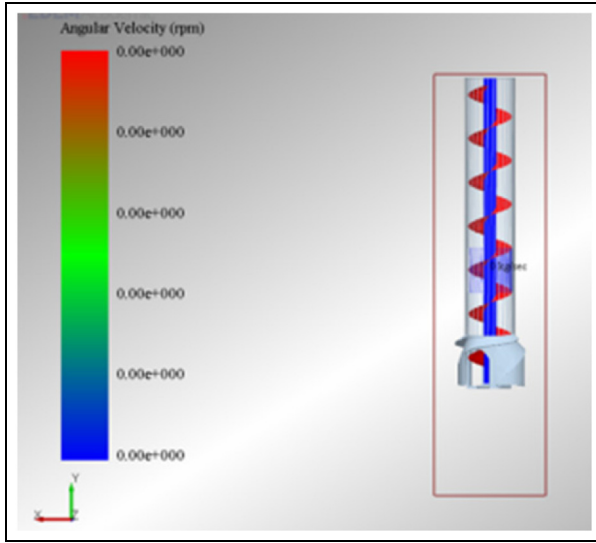


**Figure 6.** EDEM model for vertical screw conveyor.

## Design method based on TCP-SHV

### The model and calculation procedure of EDEM + FLUENT

In order to simulate the actual particles transmission, conveyor adopts method of feeding head, and the initial parameters are as follows: radius of spiral blade:  $R_2 = 0.15$  m, diameter of screw axis:  $R_1 = 0.05$  m, thickness of screw blade:  $\Delta h = 0.002$  m, pitch:  $S = 0.225$  m, and height of screw conveyor:  $h = 1.2$  m.

The model build by SOLIDWORKS software is imported in EDEM software, as shown in Figure 6. And, the model by SOLIDWORKS software also is imported in ICFM software to generate mesh, and all use unstructured grid.

The EDEM + FLUENT model constitutes of FLUENT calculation of gas phase field and EDEM calculation of particle dynamics. When simulating, to

perform solution of particle phase field and gas phase field alternately, the following specific steps are followed:

1. The gas phase flow field and particle flow field are initialized.
2. Having numerical solution to control equation of gas phase within the given time step using SIMPLEC method and obtaining the velocity field of gas phase.
3. *Solving the particle movement.* Solving the air drag force and pressure gradient force, respectively; judging whether collision between particles and particles, the wall, the screw blade occurs, and if collision occurs, calculating the impact force; then, calculating the force and moment the particles suffer and then determining the acceleration of particle collision according to Newton's second law; finally, calculating the position and speed of all particles after a time step in order to determine the motion curve of particles.
4. Updating the void fraction in the gas phase flow field grid and computing the average speed of particles in grid and calculating the reaction source term of the particle to flow field.
5. Amending the gas phase control equation and then concluding the new gas phase flow field.
6. Repeat steps (2)–(5), until the end of the step length.

The flow characteristics when a TCP-SHV flow is formed in the vertical screw conveyor were analyzed under different filling rates and different screw speeds.

### Best filling rate

The velocity vector and trajectory of the particle were obtained by conducting EDEM + FLUENT



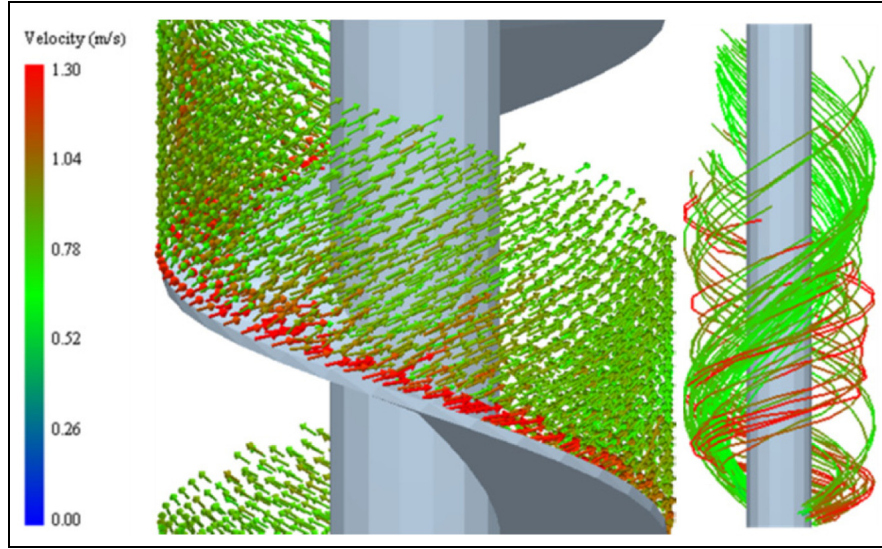
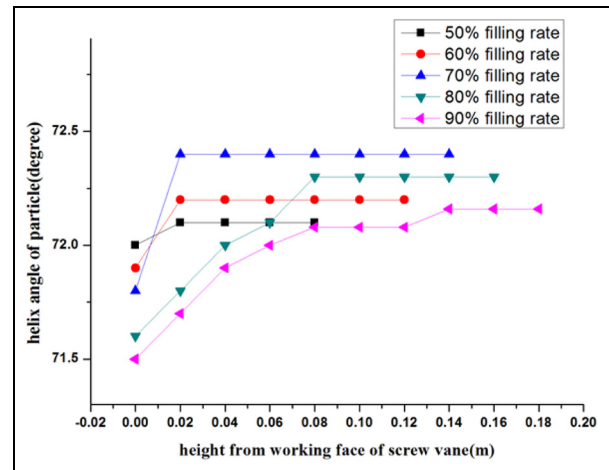


**Figure 7.** Chart for velocity vector and trajectory of particle swarm when screw speed is 500 r/min and the filling rate is 60%.

simulation analysis, as shown in Figure 7. The direction of the velocity vector of the particle group is inconsistent. At the lower strata in the particle group, that is, near the working face of the screw blade, the angle between the direction of the particle velocity and the screw blade is not large, indicating that the underlying particle has a large circumference velocity due to the restriction by the upper particles. However, the particle has a smaller upward transport speed, suggesting that the transport efficiency near the working surface of the screw blade is not high. Thus, as the height of the particle group increases, the angle between the direction of the particle velocity and the screw blade gradually increases. When the middle of the particle group is reached, the angle between the direction of the particle velocity and the screw blade no longer changes. The angle no longer changes within the upper layer of the particle group, whose velocity direction in the same diameter shows a nearly parallel characteristic.

To obtain the best filling rate, therefore, the velocity direction of the vast majority of particles of the same diameter must possess a nearly parallel characteristic.

According to Figure 1,  $\tan \lambda = V_L / V_T$ , where  $\lambda$  is the helix angle of the particle,  $v_T$  is the circumference velocity of the particle, and  $v_L$  is the vertical speed of the particle. By performing the simulation when friction is present between the particle and the screw blade for a pipe wall with friction coefficient of 0.2, the vertical velocity and circumferential velocity of the particle can be obtained at different filling rates. Accordingly, the helix angle of the particle flow can be calculated. The velocity vector direction of the particle, that is, the helix angle of the particle at different filling rates is shown in Figure 8.

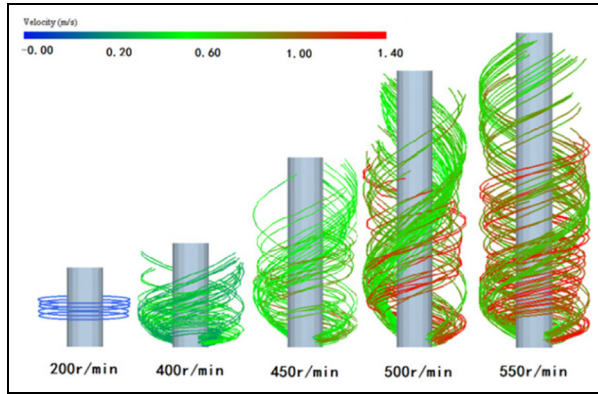


**Figure 8.** Helix angle of the particle swarm at different filling rates.

As shown in Figure 8, when the filling rate is 50%, 60%, or 70%, the velocity direction of the particle flow in the same radius is nearly the same with the exception that the velocity direction of the particle has a smaller angle on the working face of the screw blade, whose particle flow is TCP-SHV. However, when the filling rate is 80% or 90%, the lower layer of the particle flow has a small angle of velocity direction of the particle and is almost parallel to the upper layer. This phenomenon indicates that the interaction among particles is strengthened with the increase in the filling rate, which in turn destroys the TCP-SHV flow. A higher filling rate corresponds to a higher efficiency of the screw conveyor. Therefore, when the friction coefficient between the particle and the screw blade is 0.2, the friction coefficient between the particle and the pipe wall is also 0.2

**Table 3.** The best filling rate with different friction coefficients.

| Friction coefficient between the particle and the screw blade | Friction coefficient between the particle and the pipe wall | The best filling rate (%) |
|---------------------------------------------------------------|-------------------------------------------------------------|---------------------------|
| 0.1                                                           | 0.1                                                         | 50                        |
| 0.2                                                           | 0.2                                                         | 70                        |
| 0.4                                                           | 0.4                                                         | 70                        |
| 0.6                                                           | 0.6                                                         | 70                        |

**Figure 9.** Trajectory diagram of the particle at different screw speeds when the filling rate is 70%.

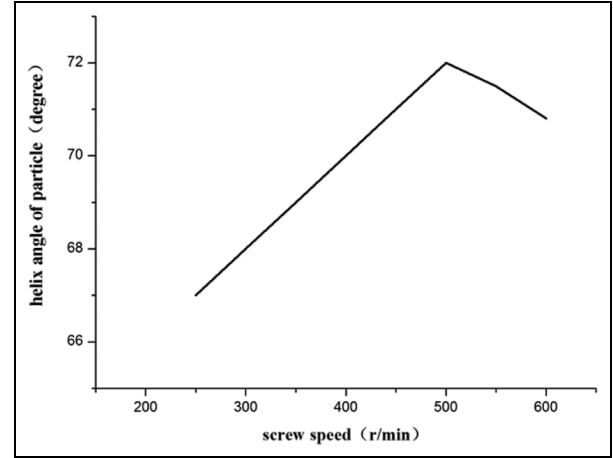
and the best filling rate of the TCP-SHV flow formed in the vertical screw conveyor is 70%.

According to the above method, the best filling rate of TCP-SHV formed in the vertical screw conveyor with different friction coefficients is as shown in Table 3.

### Best screw speed

**Analysis of the helix angle.** Figures 9 and 10 show the trajectory diagram and the helix angle diagram of the particle at different screw speeds when the filling rate is 70%.

As shown in the graph, when the screw speed is less than 200 r/min, the trajectory of the particle flow is TC flow, which manifests only circumferential movement without axial movement. When the speed exceeds 200 r/min, the trajectories of particles team with the helix, whose flow field turns into the TCP flow state. As the screw speed is increased to 200, 300, 400, and 500 r/min, the trajectory length of the particle increases, indicating that the average vertical speed of the particle flow increases. As the screw speed increases, the color of the trajectory gradually changes from blue and green into red, suggesting that the average speed of the particle flow is also increased. However, when the screw speed is further increased from 500 to 550 r/min, the growth

**Figure 10.** Helix angle diagram of the particle at different screw speeds when the filling rate is 70%.

of the trajectory length of the particles is reduced, and the helix angle decreases. Meanwhile, the speed of the particle is increased, meaning that the growth rate of the circumferential velocity of the particle is increased. The reason is that when the screw speed becomes excessively high, the particle will be thrown outward because of the extremely large centrifugal force. By this time, the TCP-SHV is no longer stable and is disturbed, and the particles are no longer being conveyed efficiently.

Thus, the flow field in the screw conveyor is TCP-SHV when the screw speed ranges from 200 to 500 r/min. A higher screw speed corresponds to a greater average vertical speed of the particle, which in turn corresponds to a higher efficiency of the screw conveyor. Therefore, when the friction coefficients between the particle and screw blade and the pipe wall both are 0.2, the best screw speed of the TCP-SHV flow formed in the vertical screw conveyor is 500 r/min.

**Analysis of the vorticity state.** In view of the roles of centrifugal force and friction, the particle flow in a vertical screw conveyor is vortex flow, causing the particle in the vertical screw conveyor to produce vorticity stream. The vorticity is defined by the angular velocity of a particle point in the particle flow, whose size represents the size of the curl in the flow field. A larger vorticity stream corresponds to a larger rotating angular velocity and, in turn, a stronger rotary motion, which is unfavorable for the vertical transport of particles. Figure 11 shows the vorticity with the changes in the screw speed.

As shown in Figure 11, when the screw speed increases from 400 and 450 to 500 r/min, the vorticity displays no significant change. However, when the screw speed increases from 500 to 550 r/min and further to 600 r/min, the vorticity stream becomes larger, indicating that the vortex intensity is increased.

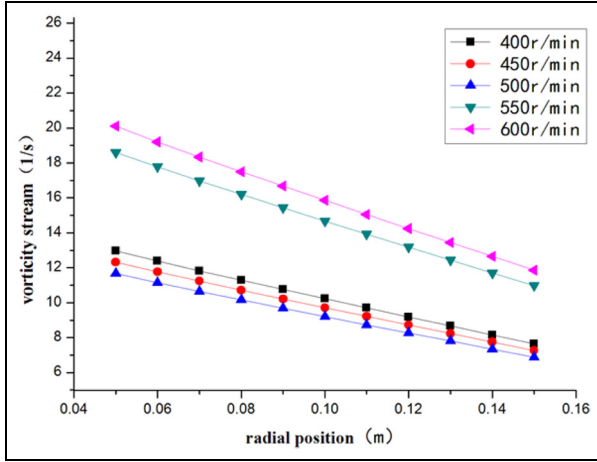


**Figure 11.** Vorticity stream with the changes in the screw speed.

Consequently, the rotary motion of particle flow is enhanced, and the particles are not being conveyed efficiently. Therefore, the best screw speed of the TCP-SHV flow formed in the vertical screw conveyor is 500 r/min; this finding is the same as the results for the analysis of the helix angle.

### Critical Reynolds number

According to formula (6), the average circumferential speed of the particle is as follows

$$\begin{aligned}\bar{v}_T &= \frac{1}{R_2 - R_1} \int_{R_1}^{R_2} v_T dr \\ &= \frac{0.08\omega(-\frac{1}{3}R_1^2 + \frac{2}{3}R_1R_2 + \frac{2}{3}R_2^2 + 0.004R_2 + 4 \times 10^{-6})}{(0.002 + R_2)^2}\end{aligned}\quad (12)$$

Substituting  $R_1 = 0.3R_2$  in the above formula yields the following

$$\bar{v}_T = \frac{0.08\omega(0.84R_2^2 + 0.004R_2 + 4 \times 10^{-6})}{(0.002 + R_2)^2}\quad (13)$$

Placing the formula of the Reynolds number in the vertical screw conveyor, the following is obtained

$$\begin{aligned}\text{Re} &= \frac{\rho \bar{v}_T d}{\mu_m} = \frac{2\bar{v}_T \rho (R_2 - R_1)}{\mu_m (R_2 - R_1 + S)} \\ &= \frac{2\bar{v}_T S \rho (R_2 - R_1)}{\mu_g (1 + 2.5\phi)(R_2 - R_1 + S)} \\ &= \frac{0.112\omega S R_2 \rho (0.84R_2^2 + 0.004R_2 + 4 \times 10^{-6})}{\mu_g (0.7R_2 + S)(0.002 + R_2)^2 (1 + 2.5\phi)}\end{aligned}\quad (14)$$

**Table 4.** The best screw speed and the critical Reynolds number.

| $\mu_1$ | $\mu_2$ | The best filling rate $\phi$ | Screw radius $R_2$ (mm) | Screw pitch $S$ (mm) | The best screw speed $\omega$ (r/min) | Critical Reynolds number (Re) |
|---------|---------|------------------------------|-------------------------|----------------------|---------------------------------------|-------------------------------|
| 0.2     | 0.2     | 0.7                          | 100                     | 150                  | 796                                   | 1903 $\rho$                   |
|         |         |                              | 150                     | 225                  | 570                                   | 2037 $\rho$                   |
|         |         |                              | 200                     | 300                  | 460                                   | 2194 $\rho$                   |
|         |         |                              | 250                     | 375                  | 400                                   | 2383 $\rho$                   |
|         |         |                              | 300                     | 450                  | 360                                   | 2569 $\rho$                   |
|         |         |                              | 400                     | 600                  | 300                                   | 2856 $\rho$                   |
|         |         |                              | 500                     | 750                  | 270                                   | 3217 $\rho$                   |

where  $\omega$  is the screw speed,  $S$  is the screw pitch (m),  $S = 1.5R_2$ ,  $R_2$  is the screw radius (m),  $\rho$  is the bulk density of the particle flow ( $\text{t/m}^3$ ),  $\mu_g$  is the coefficient of kinematic viscosity for the air,  $\mu_g = 1.8e - 5$  ( $\text{m}^2/\text{s}$ ), and  $\phi$  is the filling rate of the particle flow.

According to the preceding simulation calculation, the best screw speed of the TCP-SHV flow formed in the vertical screw conveyor is 0 and the best filling rate is 70%, and when  $R_2 = 0.15$  m,  $S = 0.225$  m, and  $\rho = 0.7$   $\text{t/m}^3$ , the friction coefficient between the particle and the screw blade is  $\mu_1 = 0.2$  and that between the particle and the pipe wall is  $\mu_2 = 0.2$ .

Substituting these parameters in formula (14), the critical Reynolds number of the TCP-SHV flow formed in the vertical screw conveyor can be obtained as follows

$$\text{Re} = 2037\rho \quad (15)$$

According to the simulation and the formula of Reynolds number, the best screw speed and the critical Reynolds number of the TCP-SHV flow formed in the vertical screw conveyor when  $\mu_1 = 0.2$  and  $\mu_2 = 0.2$  and under different screw radii are shown in Table 4.

The relationship between the critical Reynolds number and the screw radius is obtained fitting the critical Reynolds number and the screw radius, as shown in Figure 12.

By performing linear fitting for Figure 12, the linear fitting function can be obtained as follows

$$\text{Re} = \rho(3307.7R_2 + 1553.5)$$

According to the preceding analysis, the linear fitting function of the critical Reynolds number for different friction coefficients can be obtained, as shown in Table 5.

### Best throughput

Using formula (14) for the Reynolds number, the formula for the best screw speed can be expressed as follows



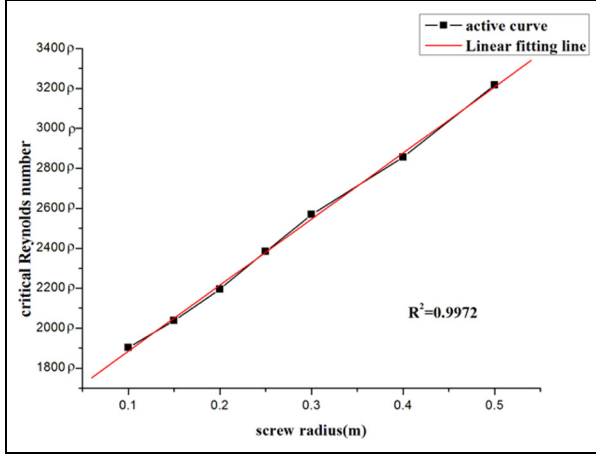


**Figure 12.** Linear fit of the critical Reynolds number.

$$\omega = \frac{Re * \mu_g(0.7R_2 + S)(0.002 + R_2)^2(1 + 2.5\phi)}{0.112SR_2\rho(0.84R_2^2 + 0.004R_2 + 4 * 10^{-6})} \quad (16)$$

Formula (16) is substituted to formula (11) for the throughput to derive the formula for the throughput of the TCP-SHV flow formed in the vertical screw conveyor as follows

$$\begin{aligned} Q &= \frac{\pi}{4}(4R_2^2 - 4R_1^2)\phi\rho v_L = 0.91\omega S\rho\phi\pi R_2^2 \\ &\left(1 - \frac{0.04(0.00684 + 1.35R_2)}{\pi(0.002 + R_2)^2}\right) \\ &= 8.125Re * \mu_g\phi R_2 * \\ &\frac{(0.7R_2 + S)(1 + 2.5\phi)(3.14R_2^2 - 0.0414R_2 - 2.61 * 10^{-4})}{(0.84R_2^2 + 0.004R_2)} \end{aligned} \quad (17)$$

where  $Q$  is the throughput (t/s);  $Re$  is the critical Reynolds number of the TCP-SHV flow formed in the vertical screw conveyor, whose data can be found in Table 4;  $S$  is the screw pitch (m),  $S = 1.5R_2$ ;  $R_2$  is the screw radius (m);  $\rho$  is the bulk density of the particle flow (t/m<sup>3</sup>);  $\mu_g$  is the coefficient of kinematic viscosity for the air,  $\mu_g = 1.8e - 5$ (m<sup>2</sup>/s); and  $\phi$  is the filling rate of the particle flow, whose data are provided in Table 1.

### Design method process

When the throughput  $Q$ , the transport height  $H$ , the packing density of the particle  $\rho$ , the friction coefficients between the particle and screw blade  $\mu_1$ , and the friction coefficients between the particle and pipe wall  $\mu_2$  are known, the design method based on TCP-SHV is as follows:

1. Using the friction coefficients  $\mu_1$  and  $\mu_2$ , search Table 3 for the best filling rate and Table 5 for the critical Reynolds number.

**Table 5.** The linear fitting function of the critical Reynolds number for different friction coefficients.

| Friction coefficient between the particle and the screw blade | Friction coefficient between the particle and the pipe wall | Critical Reynolds number (Re)   |
|---------------------------------------------------------------|-------------------------------------------------------------|---------------------------------|
| 0.1                                                           | 0.1                                                         | $Re = \rho(2481.4R_2 + 927.9)$  |
| 0.2                                                           | 0.2                                                         | $Re = \rho(3221.5R_2 + 1580.7)$ |
| 0.4                                                           | 0.4                                                         | $Re = \rho(2481.4R_2 + 927.9)$  |
| 0.6                                                           | 0.6                                                         | $Re = \rho(2481.4R_2 + 927.9)$  |

2. Input the best filling rate, the critical Reynolds number, pitch  $S = 1.5R_2$ , and bulk density into formula (17) to obtain the throughput.
3. Use formula (17) for the throughput to obtain the screw radius  $R_2$ , the pitch  $S$ , and the radius of the screw shaft.
4. Input the screw radius  $R_2$ , the pitch  $S$ , the best filling rate  $\phi$ , and the critical Reynolds number  $Re$  in formula (16) for the screw speed to obtain the best screw speed  $\omega$ .
5. In the formula  $N = QH\omega/367\eta$ , for calculating the power,  $N$  is the power of the conveyor (kW),  $Q$  is the throughput  $Q$ (t/s),  $\omega$  is the drag coefficient of the particle, whose data are chosen by experience, and  $\eta$  is the transmission efficiency of the actuating device, whose data generally are 0.9.

### Efficiency of the method

Table 6 shows the comparison of the proposed method with the design method of the vertical screw conveyor based on the material group method used in the design manual of continuous conveyor.

Using the design method of the vertical screw conveyor based on TCP-SHV in this article, the throughput of the vertical screw conveyor can be increased by 20% with the same screw radius, the same pitch, and the same particle.

### Conclusion

1. This article analyzed the speed of the particle in the vertical screw conveyor and the distribution function of circumferential speed of the particle in the radial direction. Thus, the formula for the throughput was deduced.
2. On the basis of the helix angle and vorticity of the particle flow, this article determined the best filling rate and the best screw speed of the TCP-SHV flow formed in the vertical screw conveyor.

**Table 6.** Comparison of conveying capacity.

| $\mu_1$ | $\mu_2$ | The best filling rate $\phi$ | Screw radius $R_2$ (mm) | Screw pitch $S$ (mm) | The best screw speed $\omega$ (r/min) | Throughput of traditional design method (t/h) | Throughput of the proposed method (t/h) | Increasing rate of throughput (%) |
|---------|---------|------------------------------|-------------------------|----------------------|---------------------------------------|-----------------------------------------------|-----------------------------------------|-----------------------------------|
| 0.1     | 0.1     | 0.5                          | 100                     | 150                  | 757                                   | 53                                            | 66                                      | 24                                |
|         |         |                              | 150                     | 225                  | 618                                   | 147                                           | 177                                     | 21                                |
|         |         |                              | 200                     | 300                  | 535                                   | 301                                           | 355                                     | 18                                |
|         |         |                              | 250                     | 375                  | 478                                   | 527                                           | 615                                     | 17                                |
|         |         |                              | 300                     | 450                  | 437                                   | 832                                           | 985                                     | 18                                |
|         |         |                              | 400                     | 600                  | 378                                   | 1707                                          | 2040                                    | 19                                |
| 0.2     | 0.2     | 0.7                          | 500                     | 750                  | 338                                   | 2982                                          | 3693                                    | 24                                |
|         |         |                              | 100                     | 150                  | 670                                   | 57                                            | 70                                      | 26                                |
|         |         |                              | 150                     | 225                  | 500                                   | 150                                           | 188                                     | 25                                |
|         |         |                              | 200                     | 300                  | 400                                   | 302                                           | 368                                     | 22                                |
|         |         |                              | 250                     | 375                  | 350                                   | 528                                           | 641                                     | 22                                |
|         |         |                              | 300                     | 450                  | 310                                   | 833                                           | 994                                     | 19                                |
| 0.4     | 0.4     | 0.7                          | 400                     | 600                  | 270                                   | 1711                                          | 2083                                    | 22                                |
|         |         |                              | 500                     | 750                  | 240                                   | 3042                                          | 3650                                    | 20                                |
|         |         |                              | 100                     | 150                  | 530                                   | 45                                            | 55                                      | 22                                |
|         |         |                              | 150                     | 225                  | 400                                   | 123                                           | 150                                     | 22                                |
|         |         |                              | 200                     | 300                  | 330                                   | 254                                           | 304                                     | 19                                |
|         |         |                              | 250                     | 375                  | 290                                   | 445                                           | 532                                     | 19                                |
| 0.6     | 0.6     | 0.7                          | 300                     | 450                  | 260                                   | 701                                           | 834                                     | 19                                |
|         |         |                              | 400                     | 600                  | 220                                   | 1440                                          | 1698                                    | 18                                |
|         |         |                              | 500                     | 750                  | 200                                   | 2515                                          | 3042                                    | 21                                |
|         |         |                              | 100                     | 150                  | 510                                   | 43                                            | 53                                      | 23                                |
|         |         |                              | 150                     | 225                  | 380                                   | 118                                           | 143                                     | 21                                |
|         |         |                              | 200                     | 300                  | 310                                   | 242                                           | 285                                     | 18                                |
|         |         |                              | 250                     | 375                  | 270                                   | 423                                           | 495                                     | 17                                |
|         |         |                              | 300                     | 450                  | 250                                   | 667                                           | 802                                     | 20                                |
|         |         |                              | 400                     | 600                  | 210                                   | 1369                                          | 1621                                    | 18                                |
|         |         |                              | 500                     | 750                  | 190                                   | 2392                                          | 2990                                    | 21                                |

In addition, the formula for the Reynolds number was deduced. Thus, the critical Reynolds number and the best throughput were obtained under different friction coefficients.

- This article proposed an efficient design method for the vertical screw conveyor based on TCP-SHV. This method increases the throughput of the vertical screw conveyor by 20% for the same screw radius, the same pitch, and the same particle. The proposed method is greatly beneficial for the design of the vertical screw conveyor.

### Declaration of conflicting interests

The author(s) declared no potential conflicts of interest with respect to the research, authorship, and/or publication of this article.

### Funding

The author(s) disclosed receipt of the following financial support for the research, authorship, and/or publication of this article: This research was supported by the National Natural Science Fund Project under grant no. 51575370, the Shanxi International Cooperation Project under grant no.

2015081008, the Shanxi Jincheng science and technology plan project under grant no. 201501004-7, and the Scientific and technological innovation programs of higher education institutions in Shanxi under grant no. 2017160.

### References

- Wenbin S. The optimization research and improvement of screw conveyor. *Silicon Val* 2014; 8: 179–180.
- Dongzhi X and Yuwei X. The choice and determination of design parameters of screw conveyor. *Cem Technol* 2010; 1: 29–33.
- Dong S. Direct numerical simulation of turbulent Taylor–Couette flow. *J Fluid Mech* 2007; 587: 373–393.
- Yongzhi L, Hualin B and Qiongzhu J. Research on vertical conveying procedure of screw unloader. *J Wuhan Port Waterw Eng Coll* 1992; 6: 131–136.
- Jiangai C and Wenjun M. Mobility study for bulk solid within vertical screw conveyor. *Mech Eng Autom* 2012; 6: 1–3.
- Lei M. The vertical conveying mechanism and experimental study of spiral discharging. *Wuhan Univ Technol Diss* 2014; 5: 7–10.
- Jiemei Z. The study on vertical screw conveyor process based on the material speed radial change. *Wuhan Univ Technol* 2013; 5: 4–6.

8. Mendiburua A and Carrocci LR. Analytical solution for transient one dimensional Couette flow considering constant and time-dependent pressure gradients. *Therm Eng* 2009; 8: 92–98.
9. Climenta E. Preferential accumulation of bubbles in Couette-Taylor flow patterns. *Phys Fluids* 2007; 15: 1–8.
10. Dressler M, Edwards BJ and Windhab EJ. An examination of droplet deformation and break-up between concentrically rotating cylinders. *J Non-Newton Fluid* 2008; 152: 86–100.
11. Leclercq C, Pier B and Scott J. Hydrodynamic instabilities in the eccentric Taylor-Couette-Poiseuille flow. *EUROMECH Colloq* 2011; 525: 21–23.
12. Yanping Y and Honghu J. The numerical modeling of Couette-Taylor-Poiseuille flow. *Lubr Airproof* 2006; 3: 25–28.
13. Guy Raguin L and Georgiadis JG. Kinematics of the stationary helical vortex mode in Taylor–Couette–Poiseuille flow. *J Fluid Mech* 2004; 516: 125–154.
14. Poncet S, Haddadi S and Viazzoz S. Numerical modeling of fluid flow and heat transfer in a narrow Taylor-Couette-Poiseuille system. *Int J Heat Fluid Fl* 2010; 32: 128–144.
15. Lau YL, Leung RCK and So RMC. Vortex-induced vibration effect on fatigue life estimate of turbine blades. *J Sound Vib* 2007; 307: 698–710.
16. Leung RCK, So RMC, Wang MH, et al. In-duct orifice and its effect on sound absorption. *J Sound Vib* 2007; 299: 990–1004.
17. Lau YL, So RMC and Leung RCK. Flow-induced vibration of elastic slender structures in a cylinder wake. *J Fluid Struct* 2004; 19: 1061–1083.
18. Yuhang G. Study on numerical simulation of characteristics on of gas-solid two phase flow in vertical screw conveyor. *Taiyuan Univ Sci Technol* 2015; 5: 15–20.
19. Owen PJ and Cleary PW. Prediction of screw conveyor performance using the discrete element method (DEM). *Powder Technol* 2009; 193: 274–288.
20. Xinyu S. Numerical simulation of dense phase plug flow pneumatic conveying. *Jilin Univ* 2016; 6: 22–25.
21. Xiansheng Z. The numerical simulation of gas-solid two phase flow in pneumatic conveying pipe. *South China Univ Technol* 2015; 4: 13–15.
22. Xiaoxia S and Wenjun M. The research into structure-dependent gas-solid two-phase flow within vertical screw conveyor. *Int J Multimed Ubiquitous Eng* 2017; 12: 1–14.
23. Zhanyi Z and Xiaoxia S. Distribution of particle velocity in vertical screw conveyor. *J Process Eng* 2015; 15: 909–915.